

Synthesis and characterisation of an Acid-based Iron-Metal Organic Framework for Green Hydrogen Production

Sanelisiwe Dietsela¹, Emmanuel K. Tetteh¹, Sudesh Rathilal¹, and Sampson Mamphweli¹

Abstract— South Africa as a country cannot be exempted from global industrial activities and rising population demand on fossil fuels and coal posing a great threat to the sustainability of the environment. In essence, the continuous use of fossil fuels as the primary energy source contributes significantly to ozone layer depletion and a large carbon footprint. The global shift toward sustainable energy sources is driven by an urgent need to reduce greenhouse gas emissions, in line with the United Nations Sustainable Development Goals (SDGs), notably SDG 7 (Affordable and Clean Energy) and SDG 13 (Climate Action). Therefore, exploring green hydrogen as an alternative energy source towards a carbon-neutral economy is useful.

Among the various production routes for green hydrogen, electrocatalysis has proven to be a promising technology. However, the electrocatalysis process is limited by the engineering of suitable catalysts to maximize its efficiency and by advancing this technology, South Africa's coal-dependent economy can transition to a green economy, aligning with the UN's SDG 7 and 13. Therefore, this study aimed to explore the synthesis and characterization of the Iron-Metallic Organic Framework (MOF) catalyst in an acidic medium for green hydrogen production. This involves the engineering of the MOF via a modified hydrothermal technique under an acidic condition by adjusting the pH (2-6) with sodium hydroxide.

Analytical techniques such as Brunauer-Emmett-Teller (BET), and Fourier Transform Infrared Spectroscopy (FTIR) were used to determine morphological properties (surface area, pore size, and volume), elemental composition, and functional groups respectively. The energy potential of the MOFs was estimated, to assess their viability for green hydrogen production. The BET results of the calcined Iron MOF showed a high surface area of 2551 m².g⁻¹ and a pore volume of 1.407 cm³.g⁻¹.

The uncalcined Iron MOF catalyst, however, had a lower surface area and pore volume of 1940 m².g⁻¹ and 0.54 cm³.g⁻¹. These results show the effect of calcining the catalysts, which in this case, improves their morphology. The high surface areas of the calcined Iron MOF can provide more active sites for the adsorption and stability of hydrogen molecules. This MOF has been demonstrated to be an excellent catalyst for hydrogen adsorption, helping to stabilise green hydrogen production. The prospects of this project as a feasibility study for green hydrogen production will contribute to decarbonization,

socio-economic growth, and the security of South Africa's energy mix.

Keywords— Green hydrogen, water-energy nexus, Iron-metal organic framework (MOF), electrolysis, green energy.

I. INTRODUCTION

The increased population demands more energy and fuel, which has negatively affected the environment since the combustion of fossil fuels releases greenhouse gases [1]. This energy demand is further fueled by the recent disruptions that have been taking place in South Africa, such as energy shortage issues from Eskom and Covid-19 outbreaks [2]. This energy crisis has affected many semi-developed countries in Africa, such as South Africa, as well as other countries around the world.

This underscores the need to find alternative energy sources that do not emit greenhouse gases and are cost-effective. Amongst all the other sources of cleaner energy such as biodiesel, geothermal heat, biochar, etc., green hydrogen counts as one of them. Green hydrogen is produced from renewable energy sources and does not harm the environment. This source of energy can be used in many sectors, such as transport facilities, economic sectors, and energy industries, which brings the need to produce this form of clean energy [3]. There are several techniques for producing hydrogen, such as steam reforming or coal gasification. However, these processes are costly, energy-intensive and pose a significant threat to environmental well-being. Water electrolysis offers an eco-friendlier route that involves dissociating water molecules, allowing hydrogen to be produced by adding electricity [4].

Green hydrogen has been recognised as a sustainable fuel that can phase out the use of fossil fuels; however, it requires greater attention to optimising production strategies. Despite advancements in hydrogen production technology, the challenge remains to ensure a cost-effective, commercially viable process. A promising enhancement strategy for hydrogen production using water electrolysis is the addition of a catalyst. A catalyst used in water electrolysis can stabilise hydrogen molecules, which are required for hydrogen adsorption.

The best hydrogen yield results from using platinum as a catalyst [5]. However, platinum is scarce and expensive, making it almost impossible to use it on an industrial scale. Metal-organic frameworks, however, have specific desirable

Manuscript received Sep. 26, 2025. This work was supported in part by the Durban University of Technology and Green Engineering Research Group.

¹Durban University of Technology, Durban, Steve Biko Campus, S4L1, 4001, South Africa

morphological properties, such as large surface areas and pore volumes, and diverse chemical structures, which qualify them as catalysts.

II. METHODOLOGY

This methodology outlines the synthesis, drying, calcination, and cleaning procedures for the iron-MOF catalyst. It is a chapter depicting a feasibility study of the synthesis of the Fe-MOF. Analytical methods such as FTIR, BET, and TGA are examined. The chosen methodology aims to ensure reliable and valid results. By detailing the steps taken, this section enables replication of the study and provides transparency into the research process.

The catalyst was synthesised using the following reagents and chemicals obtained from Sigma-Aldrich South Africa: Iron nitrate nonahydrate, Trimesic acid, Ethanol, Deionised water, and Sodium hydroxide.

A. Iron MOF synthesis schematic:

Schematic and equipment of the synthesis procedure is shown Fig. 5, and a detailed pictorial view is presented in Appendix

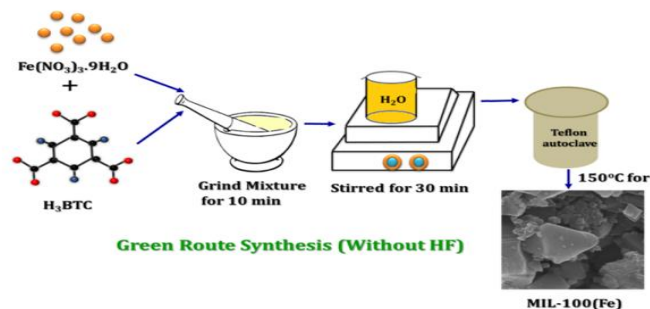


Fig 1: Schematic of synthesis procedure of modified hydrothermal method [4].

The formation of an iron-based metal-organic framework (Fe-MOF) involves the coordination of Fe^{3+} ions from iron nitrate nonahydrate with the carboxylate groups of Trimesic acid. This interaction forms secondary building units (SBUs), which then assemble into a three-dimensional porous framework [4]. The resulting structure, such as MIL-100(Fe), shown on the RHS of the figure below, features large tetrahedral and octahedral cages, providing high porosity and stability and making it suitable for catalysis.

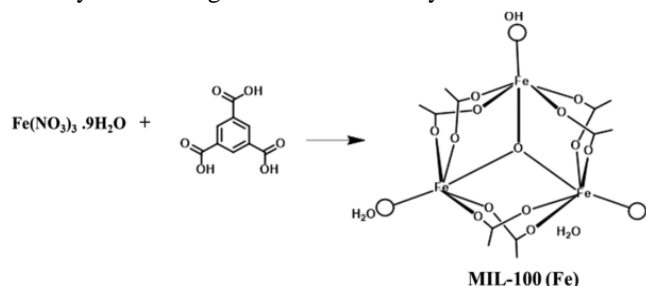


Fig 2: Schematic of the formation of the Fe-MOF [4].

III. RESULTS AND DISCUSSION

This section presents the study's findings and interprets their significance in the context of the research objectives. The results are systematically organized to highlight key observations and trends in the FTIR and TGA analyses. Following the presentation of data, a detailed discussion explores the implications of these findings, compares them with existing literature, and addresses potential limitations.

A. FTIR analysis

The summary of the FTIR spectra is presented in Table III:

TABLE III: SUMMARY OF DIFFERENT FUNCTIONAL GROUPS AT DIFFERENT WAVENUMBERS AND FREQUENCIES [6].

SL. No.	Frequency Range (cm^{-1})	Function group
1	3854	O-H stretching vibration
2	3587.12	Phenols
3	3373-3422	Bonded N-H/C-H/O-H stretching of amines and amides
4	2918.2-2954	C-H
5	2500-3300	Carboxyl acid
6	2322.8-2138.1	C-N
7	2047.30	Silicon compounds
8	1733.59	Ketones
9	1405-1445	Alkanes
10	1421-1415	C-O/C-H bending
11	1382-1036	C-O
12	1215-1325	Alkyl ketone
13	1020-1220	Alkyl amine
14	1026	Vibration of C-O in
15	469	Alkyl halides

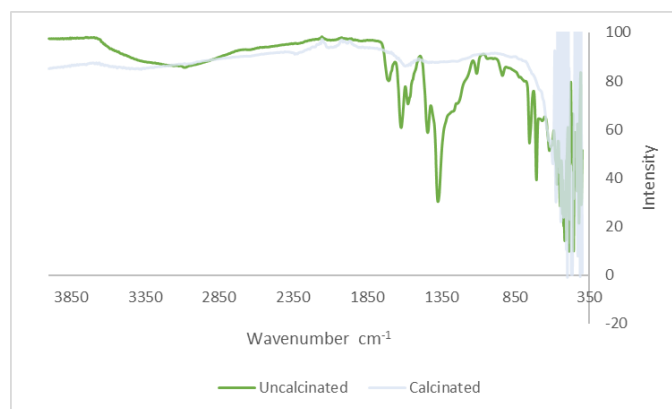


Fig 3: FTIR spectrum of Fe-MOF (calcinated and un calcinated) for the pH of 2.

Fig 7 above depicts the FTIR of an un calcinated catalyst in green and a calcinated catalyst in light blue. The results for both catalysts on the left, at wavenumbers of 2850 to 3850 cm^{-1} , depict O-H stretching in the MOF. This O-H stretching can be seen more in the un calcinated catalyst, as the vibration peaks of the catalyst are closer to it. This stretching is caused by the existence of water moieties, which are no longer present in the calcinated catalyst [7].

When a catalyst is thermally treated, processes such as desorption, dehydration, and structural changes occur [8]. During desorption, water molecules are absorbed on the catalyst surface. In dehydration, hydroxyl groups are removed through hydration process, leading to new active sites. The calcined catalyst undergoes structural changes, such as the formation of oxygen vacancies, thereby increasing its activity [9].

The stretching vibration of the double bonds between carbon and oxygen in Trimesic acid gives rise to the peak at 1850 cm^{-1} for the uncatalyzed catalyst. Low Trimesic acid intensities are expected due to the removal of residual acid. This, however, cannot be observed in the calcined sample as its structure has changed. The peaks at 1350 and 1600 cm^{-1} correspond to the symmetric and asymmetric vibrations of the COO^{-1} (carboxylate salt) group. Lastly, the peaks observed in both the calcined and uncalcined catalysts, spanning 350-850 cm^{-1} , correspond to the Fe-O stretching vibration, thus confirming that the synthesised catalyst is an Iron MOF. The above FTIR confirms the structure of the synthesised catalyst. The same structures are depicted even with the change of pH as shown in the figures below:

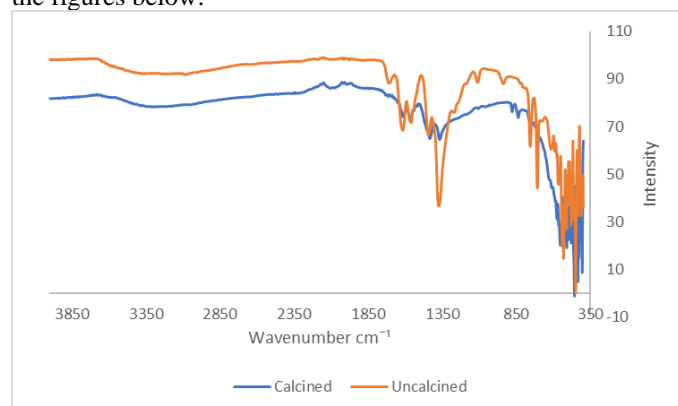


Fig 4: FTIR spectrum of Fe-MOF (calcined and un calcinated) for the pH of 4.

The diagram above depicts the same structural features as the catalysts at a pH of 2. The increase in pH, however, has increased the wavenumber of the catalysts and reduced their intensity. The calcined catalyst still shows fewer water moieties and lower vibrational bands of the residual Trimesic acid. These results are consistent with the literature and confirm the catalyst's structure and morphology.

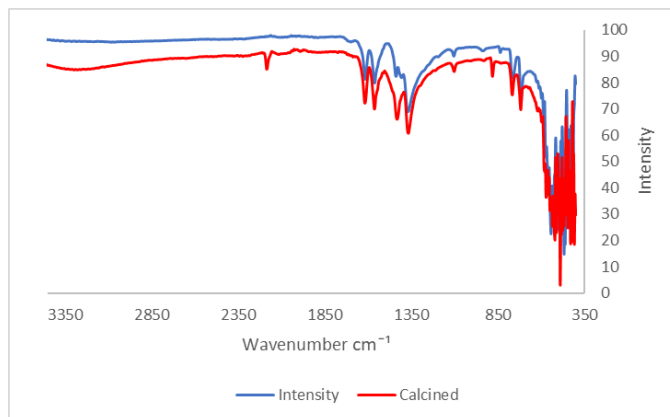


Fig 5: FTIR spectrum of Fe-MOF (calcinated and un calcinated) for the pH of 6.

The diagram above depicts the same structural features as the catalysts with the pH of 2 and pH of 4. The increase in pH to 6, however, has decreased the wavenumber of the catalysts and reduced their intensity. The calcined catalyst still shows fewer water moieties; however, the vibrations, from stretching vibrations of the double bonds to the Fe-O bonds, are the same, given that the peaks of the calcined and uncalcined catalysts are the same.

The above results are satisfactory, as they align with the literature, which states that Fe-O bond stretching occurs mostly at lower wave numbers and at low intensities, as depicted in the FTIR figures above. The literature also confirms that changing the acidity of the catalyst would result in different structures of the catalyst, which is confirmed by the changes in the wavenumbers and intensities of the FTIRs above [4]. Catalysts with a pH of 2 are recommended, as they exhibit higher wavenumbers and intensities, indicating more active sites, higher oxygen vacancies, and greater stability during hydrogen adsorption. The Summary of the functional groups identified under the different pH conditions are presented in Table 4

TABLE IV: FTIR FUNCTIONAL GROUPS AT DIFFERENT WAVELENGTHS FOR THE SYNTHESIZED CATALYST

Sample	Wavelength (cm^{-1})	Name
pH 2- Calcined	506.9179	Fe MOF halogen compound
pH 2-Uncalcined	1371	Fe MOF isopropyl group
pH 4- Calcined	451.0079	Fe MOF halogen
pH 4-Uncalcined	1371.660	Fe MOF Nitrosamine
pH 6- Calcined	1613.974	Fe MOF Diketones
pH 6-Uncalcined	488.2813	Fe MOF halogen

B. Thermogravimetric Analysis

Thermogravimetric analysis is a thermos analytical technique that measures the weight changes of a sample at a given time and temperature [10]. This analysis was performed at a constant heating rate of 3.5 to 10 $^{\circ}\text{C}$, with a final temperature of 800 $^{\circ}\text{C}$. It was done in the presence of inert nitrogen gas flowing at 10-25 mL/min. The following results show the weight changes of the calcined and un calcinated catalysts:

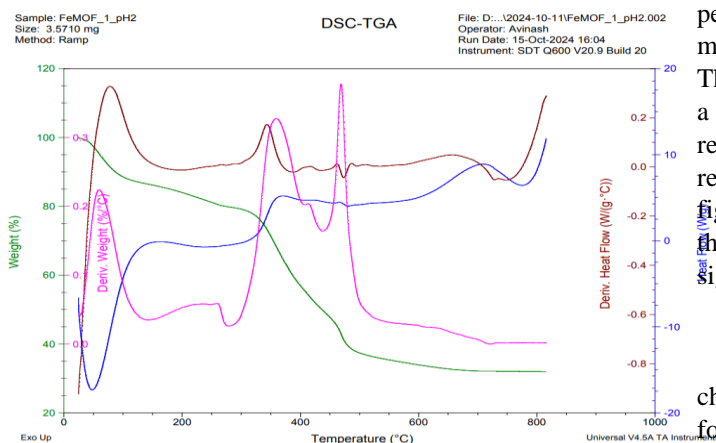


Fig 6: TGA of the synthesized, un calcinated Fe-MOF at a pH of 2.

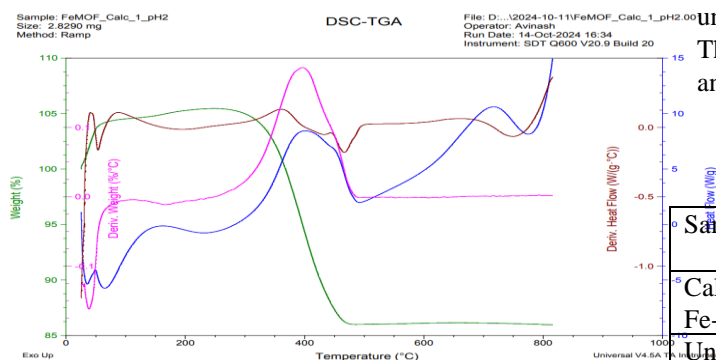


Fig 7: TGA of the synthesized, calcinated Fe-MOF at a pH of 2.

The TGA analyses of both the calcinated and uncalcinated catalysts, shown in Figs. 10 and 11 above indicate that the catalysts' weight decreases when heated. However, they are decreasing at different weight percentages. The uncalcinated catalyst loses 20.27% of its weight immediately upon exposure to heat, reaching 250°C. This is caused by the presence of hydroxyl compounds that are available in the catalyst since it was not thermally treated, showing that the catalyst corresponds to the dehydration process [10]. Since the uncalcinated catalyst did not experience dehydration in the calcination process, it will therefore lose weight faster than the calcinated catalyst. The remaining 40.73% weight loss from 250°C to 500°C corresponds to catalyst decomposition; this is where volatile gases are released, i.e., from the decomposition of organic linkers.

The calcinated catalyst does not immediately lose weight; it slightly increases from 100 to 105% and then drops down to 84%. This is a 16% weight loss of the catalyst. This explains that the uncalcinated catalyst is free from impurities and will therefore not lose weight. There is little to no catalyst decomposition, indicating that the breakdown occurred during calcination. Gases such as H₂O and carbon dioxide, or any other volatile gases in the catalyst, were released during the thermal treatment of the catalyst. The derivative weight percentage graph confirms these trends, but also shows where the significant weight% losses in the catalyst took place [10]. The peak between 350°C and 500°C in the weight derivative

percentage in Figure 10 indicates the temperatures at which the majority of the calcinated catalyst weight % is lost.

The plot above confirms that an increase in temperature leads to a decrease in catalyst weight, as reported in the literature. The remaining plots (heat flow and its derivative) depict the relationship between heat flow and the catalyst weight. The figures above show that an increase in heat flow will decrease the catalyst's weight %. The catalysts at pH 4 and 6 showed no significant changes.

C. Brunauer-Emmett-Teller analyses

The Brunauer-Emmett Teller (BET) method is used to characterise the catalyst. This analytical technique is essential for analysing catalyst properties, such as surface area, pore volume, and even pore radius. The table below shows the average volumes and surface areas of the calcinated and uncalcinated catalysts for the best catalyst, which has a pH of 2. The optimum catalyst was selected based on the FTIR results and the TGA mass loss.

TABLE V: BET RESULTS FOR THE CATALYST WITH PH OF 2.

Sample	Synthesis Process	Surface Area (m ² .g ⁻¹)	Pore Volume (cm ³ .g ⁻¹)
Calcinated Fe-MOF	Hydrothermal	2551	1.407
Uncalcinated Fe-MOF	Hydrothermal	1940	0.56

The results above depict a surface area of 2551 m².g⁻¹ for the calcinated catalyst and a lower area of 1940 m².g⁻¹ for the uncalcinated catalyst. The calcinated catalyst with the higher surface area shows that it has more active sites, enhanced reaction rate, and improved catalytic performance [11]. They are explained as follows:

- **Increased active sites:** More active sites are available for the adsorption process of hydrogen molecules; this enhances the catalyst's efficiency.
- **Enhanced reaction rate:** There is more adsorption of hydrogen molecules taking place, leading to a faster, more stable hydrogen synthesis process.
- **Improved catalytic performance:** Better distribution of catalyst material, improving the stability of the catalyst.

The higher pore volume of the calcinated Fe-MOF catalyst indicates enhanced diffusion, increased capacity, and improved mass transfer during hydrogen production. [12]. These characteristics are also explained as follows:

- **Enhanced diffusion:** Larger pores will allow the hydrogen molecules to diffuse more easily into the catalyst. Access to active sites is improved.
- **Increased capacity:** More hydrogen molecules are accommodated, which is beneficial for reactions involving large molecules.
- **Improved mass transfer:** Resistance to mass transfer is reduced by large pores, enhancing the reaction rate.

IV. CONCLUSION

A. Conclusion

The catalyst was successfully synthesized, using the hydrothermal method and procedure stated in the methodology section of this report. The pH of the catalyst was adjusted from 3 to 6. By evaluating the pH of 2, 4 and 6, it was found that the sample with the pH of 2 had the highest MOF as confirmed by the pore size and surface area of the synthesized MOF.

B. Recommendations:

Future work on the synthesis of the Fe-MOF catalyst will evaluate its energy potential by estimating the Teflon slope. SEM will be considered to analyse the surface morphology, which helps one assess the component structure. The possibility of using biocatalysis to catalyse green hydrogen production will also be explored.

ACKNOWLEDGMENT

This paper has been made possible by all my colleagues in the Green Engineering Research group (GERG) and supportive friends and family. I would therefore like to acknowledge my co-authors, Dr Emmanuel Tetteh and Professor Sudesh Rathilal, my colleagues in Green Hydrogen, Miss Ntombela and Mr Pirthraj.

REFERENCES

- [1] E. K. Tetteh, N. G. Sijadu, and S. Rathilal, "An overview of non-carbonaceous and renewable-powered technologies for green hydrogen production in South Africa: Keywords occurrence analysis," *Energy Strategy Reviews*, vol. 54, p. 101486, 2024. <https://doi.org/10.1016/j.esr.2024.101486>
- [2] N. Dyantyi-Gwanya, S. O. Giwa, T. Ncanywa, and R. T. Taziwa, "Exploring Economic Expansion of Green Hydrogen Production in South Africa," *Sustainability*, vol. 17, no. 3, 2025, doi: 10.3390/su17030901. <https://doi.org/10.3390/su17030901>
- [3] V. Panchenko, Y. V. Daus, A. Kovalev, I. Yudaev, and Y. V. Litt, "Prospects for the production of green hydrogen: Review of countries with high potential," *International Journal of Hydrogen Energy*, vol. 48, no. 12, pp. 4551-4571, 2023. <https://doi.org/10.1016/j.ijhydene.2022.10.084>
- [4] R. Nivetha *et al.*, "Highly Porous MIL-100(Fe) for the Hydrogen Evolution Reaction (HER) in Acidic and Basic Media," *ACS Omega*, vol. 5, no. 30, pp. 18941-18949, Aug 4 2020, doi: 10.1021/acsomega.0c02171. <https://doi.org/10.1021/acsomega.0c02171>
- [5] H. H. Do *et al.*, "Metal-organic-framework based catalyst for hydrogen production: Progress and perspectives," *International Journal of Hydrogen Energy*, vol. 47, no. 88, pp. 37552-37568, 2022/10/30/ 2022, doi: <https://doi.org/10.1016/j.ijhydene.2022.01.080>.
- [6] K. M. Fabelelbom, A. Saleh, M. M. Al-Tabakha, and A. A. Ashames, "Recent applications of quantitative analytical FTIR spectroscopy in pharmaceutical, biomedical, and clinical fields: A brief review," *Reviews in Analytical Chemistry*, vol. 41, no. 1, pp. 21-33, 2022. <https://doi.org/10.1515/revac-2022-0030>
- [7] N. Kotov, M. M. Keskitalo, and C. M. Johnson, "Nano FTIR spectroscopy of liquid water in the-OH stretching region," *Spectrochimica Acta Part A: Molecular and Biomolecular Spectroscopy*, vol. 330, p. 125640, 2025. <https://doi.org/10.1016/j.saa.2024.125640>
- [8] Y. Pan *et al.*, "Iron-based metal-organic frameworks and their derived materials for photocatalytic and photoelectrocatalytic reactions,"

- Coordination Chemistry Reviews*, vol. 499, p. 215538, 2024/01/15/ 2024, doi: <https://doi.org/10.1016/j.ccr.2023.215538>.
<https://doi.org/10.1016/j.ccr.2023.215538>
- [9] S. Muratović *et al.*, "Impact of dehydration and mechanical amorphization on the magnetic properties of Ni (ii)-MOF-74," *Journal of Materials Chemistry C*, vol. 8, no. 21, pp. 7132-7142, 2020. <https://doi.org/10.1039/D0TC00844C>
 - [10] J. Rami, C. Patel, C. Patel, and M. Patel, "Thermogravimetric analysis (TGA) of some synthesized metal oxide nanoparticles," *Materials Today: Proceedings*, vol. 43, pp. 655-659, 2021. <https://doi.org/10.1016/j.matpr.2020.12.554>
 - [11] S. Karmakar, M. Mukherjee, P. Bhattacharya, S. Neogi, and S. De, "Mechanistic insights into the antibacterial property of MIL-100 (Fe) metal-organic framework," *Journal of Environmental Chemical Engineering*, vol. 12, no. 3, p. 113088, 2024. <https://doi.org/10.1016/j.jece.2024.113088>
 - [12] X. Xu, H. Sun, S. P. Jiang, and Z. Shao, "Modulating metal-organic frameworks for catalyzing acidic oxygen evolution for proton exchange membrane water electrolysis," *SusMat*, vol. 1, no. 4, pp. 460-481, 2021. <https://doi.org/10.1002/sus.2.34>



Sanelisiwe Dietsela received the Bachelor of Engineering Technology degree in Chemical Engineering from Durban University of Technology, Durban, South Africa, in 2023, and the Bachelor of Engineering Technology (Honors) degree in Chemical Engineering from the same institution in 2024. She is currently pursuing the Master of Engineering degree in Chemical Engineering at Durban University of Technology, with research focused on photocatalytic green hydrogen production using engineered metal-organic frameworks (MOFs). She worked as a Chemical Engineering Tutor at Durban University of Technology for one year and has served as a Postgraduate Representative for students. She presented her research on "Green catalysis: Synthesis of Metal Organic Frameworks for green hydrogen" at the SANEDI Conference (2024) and at the DUT Faculty Research Day (2024), where she received the Best Presenter Award. Her research interests include photocatalysis, metal-organic frameworks, and sustainable hydrogen production technologies. Ms Dietsela received the Merit Award for Best Performing Student in Process Control in 2023. She continues to contribute to student leadership, mentorship, and project-based learning initiatives within chemical engineering.